Nanotechnology

Synthetic domain walls in [TbFeGa/TbFe]₂ multilayers

To cite this article before publication: Pablo Bartolome *et al* 2020 *Nanotechnology* in press https://doi.org/10.1088/1361-6528/ab8fe7

Synthetic domain walls in [TbFeGa/TbFe]$_2$ multilayers

Pablo Bartolomé[1], and Rocío Ranchal[1,2]*

[1]*Dpto. Física de Materiales, Facultad de Ciencias Físicas. Universidad Complutense de Madrid. Ciudad Universitaria s/n, Madrid 28040, Spain.*

[2]*Instituto de Magnetismo Aplicado, UCM-ADIF-CSIC, Las Rozas, Spain.*

Abstract

Here we report the possibility of creating synthetic domain walls in nominal [$Fe_{72}Ga_{28}$/$Tb_{33}Fe_{67}$]$_2$ multilayers. The magnetization as a function of the temperature reveals the absence of Compensation temperature in the samples which can be understood considering an interdiffusion process that results in the formation of TbFeGa alloys at the nominal FeGa layers. Therefore, samples are actually comprised of TbFeGa and TbFe layers. The hysteresis loops exhibit magnetization steps related to the nucleation of domain walls formed because of the competition between different interactions: i) the antiferromagnetic exchange coupling between the heavy rare earth (Tb) and the transition magnetic metal (Fe) inside each layer, ii) the antiferromagnetic coupling between Tb and Fe at the interfaces, and iii) the Zeeman energy. In good agreement with the experimental values, the nucleation field of the domain walls has been theoretically calculated taking into account the tilt of the magnetization with respect to the sample plane. Our experimental results indicate that by a proper thickness adjustment, it can be tuned both, the value of the nucleation field, and the layer in which this firstly occurs. Experimental values for the exchange bias field have also been calculated.

***Corresponding author.**

Dr. R. Ranchal

Dpto. Física de Materiales, Facultad de CC. Físicas. Ciudad Universitaria s/n

Madrid 28040, Spain

rociran@ucm.es

1. Introduction

It is believed that domain walls (DWs) will play a crucial role on the next generation of magnetic technology as for example in the fields of magnetic storage, and control of spin-polarized currents [1-4]. Whatever the application, it is compulsory to control the formation of the DWs. Heavy rare-earths (REs) such as Gd and Tb, antiferromagnetically couple with ferromagnetic transition metals (TMs) as Fe, Co, Ni, and their alloys: FeCo, FeNi, etc. [5-8]. When combined heavy REs and TMs, there are obtained ferrimagnetic (FI) systems due to the antiparallel coupling between their magnetic moments [6-8]. At low temperature, the magnetic moment of the RE is higher than that of the TM. Then, to minimize the Zeeman energy the magnetic moment of the RE is aligned in the direction of the applied magnetic field, whereas the magnetic moment of the TM is in the opposite due to the antiferromagnetic (AFM) exchange interaction between them. This is the so-called RE-dominated state [9-11]. When the temperature increases, it can be observed the Compensation temperature (T_{Comp}) at which the net magnetization is null because magnetic moments of TM and RE are equal but have opposite directions [12]. For temperatures above T_{Comp}, the magnetic moment of the TM is aligned in the direction of the applied magnetic field, and that of the RE in the opposite. This is the TM-dominated state [9-11]. Depending on the composition, growth conditions, or layer thickness, T_{Comp} in RE-based systems can be absent [5, 9, 11, 13-15]. In that case, the system is TM-dominated in the whole studied temperature range.

Theoretical and experimental works showed that the interfacial coupling in RE/TM multilayers can create magnetic structures as DWs due to the competition between the interfacial AFM exchange interaction and Zeeman energy [7-8, 14, 16-18]. In fact, there is a renewed interest in both RE-based multilayers and alloys, since they can be used to artificially create synthetic antiferromagnets [19-22], and even more interestingly, topologically stabilized DWs [23-24]. However, it is important to noteworthy that the interdiffusion that has been vastly reported in different RE-based systems can largely affect the interfacial exchange interaction and the magnetic properties of the ferrimagnetic layers [5, 11, 13, 15, 25-27].

Taking into account all these considerations, we propose a multilayer system to create stable and controlled DWs. We have studied nominal [$Fe_{72}Ga_{28}$(x nm)/$Tb_{33}Fe_{67}$(50 nm)]$_2$ multilayers in which x has been 25 and 50 nm. However, due to the interdiffusion inside the heterostructures the studied samples are [TbFeGa/TbFe]$_2$. The [$Tb_{19}Fe_{81}$/$Tb_{36}Fe_{64}$] system exhibit a hard magnetic Fe-dominated interfacial layer due to the interdiffusion [11]. In that case, the magnetization is perpendicular to the sample plane, and the role of the DWs on the magnetic behaviour has been in detail investigated [11]. In comparison to that previous work, in our studied multilayers the magnetization is mostly in the sample plane although with a small tilt towards the out of plane direction. There is an AFM coupling between Tb and Fe inside each layer, and an AFM coupling between Tb and Tb at the interface, apart from the Zeeman interaction when a magnetic field is applied. The nucleation fields (H_n) for the DWs have been theoretically calculated in good agreement with experimental values.

2. Experimental techniques

Samples were grown by the DC magnetron sputtering technique at room temperature on glass substrates. The deposition was carried out in oblique incidence with an angle between the vapor beam and the perpendicular to the sample of about 25° [28]. The nominal structure of the samples is: Mo(20 nm)/[$Fe_{72}Ga_{28}$(x nm)/$Tb_{33}Fe_{67}$(50 nm)]$_2$/Mo(20 nm) in which TbFe is 50 nm, and FeGa is 25 and 50 nm. For the Mo capping and buffer layers we have used an Ar pressure of $3 \cdot 10^{-3}$ mbar and a DC growth power of

90 W. All FeGa layers were deposited from a target with a composition of $Fe_{72}Ga_{28}$ using an Ar pressure of $3{\cdot}10^{-3}$ mbar and a DC growth power of 50 W. For the TbFe layers we have used a $Tb_{33}Fe_{67}$ target, and the same Ar pressure and power as for the FeGa layers.

Hysteresis loops were measured in a superconducting quantum interference device (SQUID) magnetometer with the applied magnetic field in the sample plane. Samples were cooled down at zero field from room temperature to the temperature at which the hysteresis loop was recorded. The magnetization as a function of the temperature was measured during the warming-up with an applied magnetic field of 100 Oe. In this case, the samples were cooled-down under an applied magnetic field of 2 kOe.

3. Results and discussion

According to the work of Mimura et al. [12], $Tb_{33}Fe_{67}$ has a T_{Comp} higher than 300 K and therefore, in the M (T) curves it might be expected a constant increase of the magnetization as the temperature is reduced from 300 K to 10 K. There is an increase of the magnetization when the temperature decreases from 300 K to around 250 K that can be related to the Curie temperature of the TbFe layers (Fig. 1), but we do not observe in the magnetization curves the behavior expected for $Tb_{33}Fe_{67}$ layers. Nominal FeGa has not T_{Comp} since it is a ferromagnet. Interdiffusion has already been reported in RE-based systems such as, Co/Gd and $Tb_{19}Fe_{81}$/$Tb_{36}Fe_{64}$ multilayers [5, 11]. In particular, interdiffusion has also been observed in [$Fe_{72}Ga_{28}$/$Tb_{33}Fe_{67}$] multilayers [25]. In that case, the interdiffusion promoted that 50 nm-thick TbFe layers sputtered from a $Tb_{33}Fe_{67}$ target only had a Tb content of around 20 at. % [25], whereas a Tb amount ca. 11 at. % interdiffused towards the FeGa given rise to TbFeGa layers. Since we have also deposited TbFe from a $Tb_{33}Fe_{67}$ target, it is therefore expected the same Tb interdiffusion as in reference [25]. In fact, the magnetization curves as a function of the temperature are similar to those presented in previous works with TbFe layers with a Tb content ca. 20 at. % [9,11-12]. Thus, TbFe layers actually have a $Tb_{80}Fe_{20}$ composition, and the nominal FeGa layers are $Tb_{10}Fe_{65}Ga_{25}$, and the studied samples are [$Tb_{10}Fe_{65}Ga_{25}$(*x* nm)/$Tb_{80}Fe_{20}$(50 nm)]$_2$. This also explains the behavior observed in the M (T) curves in which it has not been observed the expected T_{Comp} (Fig. 1). In fact, according to ref [12], TbFe alloys with a Tb content slightly below 20 at. % will not have T_{Comp}. This will be in agreement with our experimental results in which no T_{Comp} has been observed being TbFe and TbFeGa Fe-dominated in the whole studied temperature range.

In heterostructures with exchange coupling at the interfaces, the magnetic configuration can be rather complex since there is a competition between Zeeman and exchange energies [7-8, 14, 16], and a DW with a certain energy (γ) can be created at the interfaces [18, 29]. In our samples, apart from the AFM exchange interaction at the interfaces, there is also an AFM exchange interaction between Tb and Fe inside each layer, TbFe and TbFeGa, that can affect the formation of DWs.

In the hysteresis loops measured at 10 K, we can observe two magnetization steps related to the nucleation of two DWs when the applied magnetic field is reduced from the saturation state (Fig. 2a). S. Mangin et al. [30] correlate this kind of magnetization steps that do not depend on the temperature to the nucleation of DWs. In our study, the absence of influence of the temperature on the magnetization steps confirms that they are related to the DWs nucleation (Fig. 3).

In all cases, the first DW is formed in the layer with the lowest nucleation field (TbFeGa or TbFe), and the second DW in the other. In fig. 2b is schematically sketched the situation in which the first DW is nucleated in the TbFeGa, and the second in the TbFe. We present in a lateral view one interface for the shake of clarity, and the length of the arrows is a way to simply show the rotation of the magnetic moments that form the DW.

The general expression for the DW nucleation field (H_n) is given by:

$$H_n = \frac{\gamma}{2M_s(t-\delta)} \quad (1)$$

where $\gamma = 4\sqrt{AK}$ is the energy per unit area related to the formation of the DW, $\delta = \pi\sqrt{A/K}$ is the length of the DW, M_s is the saturation magnetization, and t is the thickness of the layer in which the DW is nucleated [30].

In the [TbFeGa/TbFe] multilayers studied in this work it has already been reported a tilt angle of the magnetization with respect to the sample plane (θ) of around 25° [31]. Therefore, it is necessary to introduce this tilt in the expression of the nucleation field:

$$H_n = \frac{\gamma}{2M_s(t-\delta)cos\theta} \quad (2)$$

It is important to noteworthy that the tilt of the magnetization cannot be considered as a drawback since tilted magnetic materials can be included in magnetoresistive structures or spin transfer torque devices due to their lower switching time [32-35].

DWs are also affected by the exchange interaction at the interface [36]. Therefore, it is necessary to add a term in the nucleation field that considers the AFM interfacial exchange coupling (H_{ex}):

$$H_{ex} = \frac{J}{Mtcos\theta} \quad (3)$$

where J is the exchange interaction that can be taken as 0.4 erg/cm^2. We have also introduced in expression (3) the term $cos\theta$ because of the tilt of the magnetization. Therefore, the nucleation field (H_n) for the DWs in our system is:

$$H_n = \frac{\gamma}{2M_s(t-\delta)cos\theta} + \frac{J}{M_s tcos\theta} \quad (4)$$

For TbFe we have considered $K_{TbFe} = 3\cdot10^6$ erg/cm^3, and $A_{TbFe} = 1\cdot10^{-7}$ erg/cm [12]. For TbFeGa, $A_{\mathrm{TbFeGa}} = 8\cdot10^{-8}$ erg/cm is extracted from the work of Mimura et al.

[12], whereas M_{TbFeGa} = 500 emu/cm^3, and K_{TbFeGa} = $4\cdot10^5$ erg/cm^3 have been inferred from experimental values [37-38]. In table I we present the calculated H_n for each layer by using expression (4). Some conclusions can be extracted after comparing these theoretical values with the two experimental nucleation fields observed in the left region of each hysteresis loop ($H_{n,1}$ and $H_{n,2}$ in fig. 2a). First of all, the agreement between the experimental and theoretical values is pretty good. In the multilayer with a TbFeGa thickness of 25 nm, we can correlate $H_{n,1}$ (0.5 kOe) to the nucleation field of a DW in the TbFe (H_n = 0.5 kOe), and $H_{n,2}$ (1.0 kOe) to the DW formed in the TbFeGa (H_n = 1.0 kOe). In the multilayer with a TbFeGa of 50 nm, $H_{n,2}$ = 0.5 kOe can be correlated to the TbFe, whereas $H_{n,1}$ = 0.3 kOe is related to the nucleation in the TbFeGa with a theoretical H_n = 0.4 kOe. Therefore, by an appropriate adjustment of both, TbFeGa and TbFe thicknes, we can tune H_n, and the layer in which the DW is firstly nucleated.

Reducing the magnetic field from the saturation state after the DW formation produces a shift of the hysteresis loop in the horizontal axis that can be quantified by means of the exchange-bias field (H_E). Different papers have reported about the existence of an exchange-bias effect in multilayers with a DW at the interface [18, 39-41]. This exchange-bias phenomenon does not need a field cooling process, and its sign depend on the sign of the exchange interaction at the interface. The multilayer with a TbFeGa thickness of 25 nm exhibits a large H_E of -475 Oe at 10 K (Fig. 4). The negative sign of the exchange bias field is in agreement with the fact that both, TbFeGa and TbFe, are Fe-dominated with an AFM coupling between them [11]. Following the work of Canet and coworkers [18], H_E can be calculated thanks to the expression:

$$H_E = -\frac{\pi\sqrt{2A_{min}(2M_{s,min}H+K_{min})}}{2M_{s,min}t} \quad (5)$$

where A_{min}, M_{min}, and K_{min} are those for the layer with the lowest $M_s\cdot t$ factor. We have modified the expression (5) in order to consider the tilt of the magnetization with respect to the sample plane by introducing $\cos\theta$. This modification is necessary since the perpendicular hysteresis loop shows H_E = -144 Oe, that reflects the existence of this tilt of the magnetization. Therefore, we propose the following equation to calculate H_E in our multilayers:

$$H_E = -\frac{\pi\sqrt{2A_{min}(2M_{s,min}H\cos\theta + K_{min}\cos\theta)}}{2M_{s,min}t} \tag{6}$$

In table III we summarize the experimental and theoretical H_E values obtained in the studied samples. For the theoretical value we have considered that the $M_s{\cdot}t$ factor is smaller for the TbFeGa. As it can be seen in table III, there is an excellent agreement between experimental and theoretical values.

If we anneal the layers at 400 °C for one hour, the interdiffusion is further enhanced. Hysteresis loops at 10 K reflect the detrimental effect that the thermal treatment has on the magnetic properties since DW nucleation is no longer so evident, and H_E is greatly reduced (Fig. 4).

4. Conclusions

The key point of this work is to show how the [TbFeGa/TbFe] system can be used to nucleate DWs in a controlled way. The DW nucleation magnetic field depend on the AFM exchange interaction inside the layers, the AFM interfacial exchange interaction, and the Zeeman energy. We have also found the necessity of considering the tilt of the magnetization to correctly calculate the nucleation fields. By a proper thickness adjustment, it can be tuned the value of the nucleation fields, and the layer in which this firstly occurs. In addition, there is an exchange-bias effect due to the interfacial coupling that has been also well calculated. Our experimental results pave the way to new spintronic devices with tilted magnetization in which DWs nucleation can be tuned.

Acknowledgements

We thank ‘CAI Técnicas Físicas’ of UCM for SQUID measurements. We also thank ICTS-Instituto of Sistemas Optoelectrónicos y Microtecnología (ISOM) for using some of its facilities. This work has been financially supported through the projects MAT2015-66888-C3-3-R of the Spanish Ministry of Economy and Competitiveness (MINECO/FEDER), and RTI2018-097895-B-C43 of the Spanish Ministry of Science, Innovation, and Universities.

References

[1] Parkin S S P, Hayashi M and Thomas L 2008 Magnetic domain-wall racetrack memory, *Science* **320** 190.

[2] Hayashi M, Thomas L, Rettner C, Moriya R and Parkin S S P 2007 Direct observation of the coherent precession of magnetic domain walls propagating along permalloy nanowires *Nat. Phys.* **3** 21.

[3] Woo S, Delaney T and Beach G S D 2017 Magnetic domain wall depinning assisted by spin wavebursts *Nat. Phys.* **13** 448.

[4] Milano G, Luebben M, Ma Z, Dunin-Borkowski R, Boarino L, Pirri C F, Waser R, Ricciardi C and Valov I 2018 Self-limited single nanowire systems combining all-in-one memristive and neuromorphic functionalities *Nature Comm.* **9** 5151.

[5] Colino J, Andrés J P, Riveiro J M, Martínez J L, Prieto C and Sacedón J L 1999 Spin-flop magnetoresistance in Gd/Co multilayers *Phys. Rev. B* **60** 6678-6684.

[6] Morales R, Martín J I and Alameda J M 2004 Domain walls and macroscopic spin-flip-like metamagnetism in $Gd_xCo_{1-x}/Gd_yCo_{1-y}$ exchange-coupled double layers *Phys. Rev. B* **70** 174440.

[7] Camley R E and Tilley D R 1988 Phase transitions in magnetic superlattices *Phys. Rev. B.* **37** 3413-3421.

[8] Camley R E 1989 Properties of magnetic superlattices with antiferromagnetic interfacial coupling: Magnetization, susceptibility, and compensation points *Phys. Rev. B* **39** 12316-12319.

[9] Schubert C, Hebler B, Schletter H, Liebig A, Daniel M, Abrudan R, Radu, F and Albrecht M 2013 Interfacial exchange coupling in Fe-Tb/[Co/Pt] heterostructures *Phys. Rev. B* **87** 054415.

[10] Canet F, Mangin S, Bellouard C, Piecuch M and Schuhl A 2001 Exchange bias phenomena in ferrimagnetic based bilayers *J. Appl. Phys.* **89** 6916.

[11] Hebler B, Reinhardt P, Katona G L, Hellwig O and Albrecht M 2017 Double exchange bias in ferrimagnetic heterostructures *Phys. Rev. B* **95** 104410.

[12] Mimura Y, Imamura N, Kobayashi T, Okada A and Kushiro Y 1978 Magnetic properties of amorphous alloy films of Fe with Gd, Tb, Dy, Ho, or Er *J. Appl. Phys.* **49** 1208-1215.

[13] Hebler B, Hassdenteufel A, Reinhardt P, Karl H and Albrecht M 2016 Ferrimagnetic Tb-Fe alloy Thin Films: composition and Thickness Dependence of Magnetic Properties and all-Optical switching *Front. Mater.* **3** 8.

[14] Ranchal R, Aroca C and López E 2008 Domain walls and exchange-interaction in Permalloy/Gd films *New J. Phys*. **10** 013013.

[15] Ranchal R, Aroca C, Sanchez M C, Sanchez P and López E 2006 Improvement of the structural and magnetic properties of Permalloy/Gadolinium multilayers with Mo spacers *Appl. Phys. A* **82** 697-701.

[16] Prieto J L, van Aken B B, Burnell G, Bell C, Evetts J E, Mathur N and Blamire M G 2004 Transport properties of sharp antiferromagnetic boundaries in Gd/Fe multilayers *Phys. Rev. B* **69** 054436.

[17] Cherifi K, Dufour C, Bauer Ph, Marchal G and Mangin P 1991 Experimental magnetic phase diagram of a Gd/Fe multilayered ferrimagnet *Phys. Rev. B* **44** 7733-7736.

[18] Canet F, Mangin S, Bellouard C, Piecuch M and Schuhl A 2001 Exchange bias phenomena in ferrimagnetic based bilayers *J. Appl. Phys.* **89** 6916.

[19] Blasing R, Ma T P, Yang S H, Garg C, Dejene F K, N'Diaye A T, Chen G, Liu K and Parkin S S P 2018 Exchange coupling torque in ferrimagnetic Co/Gd bilayer maximized near angular momentum compensation temperature *Nature Comm.* **9** 4984.

[20] Siddiqui S A, Han J, Finley J T, Ross C A and Liu L 2018 Current-Induced Domain Wall Motion in a Compensated Ferrimagnet *Phys. Rev. Lett.* **121** 057701.

[21] Bansal R, Chowdhury N and Muduli P K 2018 Proximity effect induced enhanced spin pumping in Py/Gd at room temperature *Appl. Phys. Lett.* **112** 262403

[22] Lapa P N, Ding J J, Pearson J E, Novosad V, Jiang J S and Hoffmann A 2017 Magnetization reversal in Py/Gd heterostructures *Phys. Rev. B* **96** 024418.

[23] Fust S, Mukherjee S, Paul N, Stahn J, Kreuzpaintner W, Böni P and Paul A 2016 Realizing topological stability of magnetic helices in exchange-coupled multilayers for all-spin-based system *Sci. Rep.* **6** 33986.

[24] Paul A, Mukherjee S, Kreuzpaintner W and Böni P 2014 Exchange-bias-like coupling in a ferrimagnetic Fe/Tb multilayer *Phys. Rev. B* **89** 144415.

[25] Ranchal R and González-Martín V 2011 Investigation on the structural and magnetic properties of sputtered $TbFe_2/Fe_3Ga$ heterostructures *J. Appl. Phys.* **110** 053901.

[26] Kim J, Lee D, Lee K J, Ju B K, Koo H C, Min B C and Lee O 2018 Spin-orbit torques associated with ferrimagnetic order in Pt/GdFeCo/MgO layers *Sci. Rep.* **8** 6017.

[27] González J A, Andrés J P, Arranz M A, López de la Torre M A and Riveiro J M 2002 Electrical resistivity and interdiffusion in $Gd_{1-x}Co_x$/Co Multilayers *J. Appl. Phys.* **92**, 914.

[28] Muñoz-Noval A, Ordóñez-Fontes A and Ranchal R 2016 Influence of the sputtering flow regime on the structural properties and magnetic behavior of Fe-Ga thin films (Ga ~ 30 at.%) *Phys. Rev. B* **93** 214408.

[29] Mangin S, Thomas L, Montaigne F, Lin W, Hauet T and Henry Y 2009 Angle dependence of the interface magnetic configuration in a model antiferromagnetically coupled ferrimagnetic/ferrimagnetic bilayer GdFe/TbFe *Phys. Rev. B* **80** 224424.

[30] Mangin S, Marchal G, Bellouard C, Wernsdorfer C and Barbara B 1998 Magnetic behavior and resistivity of the domain-wall junction GdFe(1000 Å)/TbFe/GdFe(500 Å). *Phys. Rev. B* **58** 2748.

[31] Bartolomé P, Maicas M, Biskup N, Varela M and Ranchal R 2018 Investigation of the out of plane component of the magnetization of $[Fe_{72}Ga_{28}$(x nm)/$Tb_{33}Fe_{67}$(50 nm)$]_2$ multilayers *Phys. Status Sol. A* **215** 1800183.

[32] Zha C L, Fang Y Y, Nogués J and Akerman J 2009 Improved magnetoresistance through spacer thickness optimization in tilted pseudo spin valves based on $L1_0$ (111)-oriented FePtCu fixed layers *J. Appl. Phys.* **106** 053909.

[33] You L, Lee Y O, Bhowmik D, Labanowski D, Hong J, Bokor J and Salahuddin S 2015 Switching of perpendicularly polarized nanomagnets with spin orbit torque without an external magnetic field by engineering a tilted anisotropy *PNAS* **112** 10310-10315.

[34] Krivorotov I N, Emley N C, Sankey J C, Kiselev S I, Ralph D C and Buhrman R A 2005 Time-Domain Measurements of Nanomagnet Dynamics Driven by Spin-Transfer Torques *Science* **307** 228-231.

[35] Kiselev S I, Sankey J C, Krivorotov I N, Emley N C, Schoelkopf R J, Buhrman R A and Ralph D C 2003 Microwave oscillations of a nanomagnet driven by a spin-polarized current *Nature* **425** 380-383.

[36] Zárate L, Quirós C, Vélez M, Rodríguez-Rodríguez G, Martín J I and Alameda J M 2006 Interlayer coupling mechanisms in amorphous Co_xSi_{1-x} /Si multilayers *Phys. Rev. B* **74** 014414.

[37] Ranchal R, Fin S, Bisero D and Aroca C 2014 Tailoring the magnetic anisotropy and domain patterns of sputtered TbFeGa alloys *J. Alloys Compnd.* **582** 839-843.

[38] Ranchal R and Gutiérrez-Díez V 2013 Perpendicular magnetic anisotropy in TbFeGa ternary alloys grown by cosputtering *Thin Solid Films* **534** 557-560.

[39] Mangin S, Marchal G and Barbara B 1999 Evidence of Exchange-Bias-Like Phenomenon in GdFe/TbFe/GdFe Domain Wall Junctions *Phys. Rev. Lett* 21 4336-4339.

[40] Canet F, Mangin S, Bellouard C and Piecuch 2000 Positive exchange bias in ferromagnetic-ferrimagnetic bilayers: FeSn/FeGd *Europhys. Lett.* **52** 594-600.

[41] Canet F, Bellouard C, Mangin S, Chatelain C, Senet C, Siebrecht R, Leiner V and Piecuch M 2003 Exchange bias like effect induced by domain walls in FeGd/FeSn bilayers *Eur. Phys. J. B* **34** 381-394.

Table I. Theoretical nucleation fields (H_n) calculated by means of the expression (4), for each layer.

Thickness for each layer	H_n (kOe)
TbFeGa. 25 nm	1.0
TbFeGa. 50 nm	0.4
TbFe. 50 nm	0.5

Table II. Experimental values ($H_{n,1}$ and $H_{n,2}$) for the nucleation fields observed in each sample.

Sample	$H_{n,1}$ (kOe)	$H_{n,2}$ (kOe)
$[TbFeGa(25\ nm)/TbFe(50\ nm)]_2$	0.5	1.0
$[TbFeGa(50\ nm)/TbFe(50\ nm)]_2$	0.3	0.5

Table III. Experimental and theoretical values calculated by means of expression (6) for H_E at 10 K.

Sample	$H_{E,experimental}$ (Oe)	$H_{E,theoretical}$ (Oe)
$[TbFeGa(25\ nm)/TbFe(50\ nm)]_2$	-475	-428
$[TbFeGa(50\ nm)/TbFe(50\ nm)]_2$	-196	-214

Figure captions

Figure 1. Magnetization as a function of the temperature for [TbFeGa(*x* nm)/TbFe(50 nm)]$_2$ with (○) x = 25 nm, and (●) x = 50 nm.

Figure 2. (a) Hysteresis loops recorded at 10 K for [TbFeGa(*x* nm)/TbFe(50 nm)]$_2$ with (○) x = 25 nm, and (●) x = 50 nm. $H_{n,1}$ and $H_{n,2}$ identified the first and second nucleation fields for the DWs. (b) Scheme of the DW nucleation processes in the case the first nucleation takes place in the TbFeGa layer. t_{TbFeGa} and t_{TbFe} are the layer thickness, whereas δ_{TbFeGa} and δ_{TbFe} are the DW thickness for TbFeGa and TbFe, respectively. The scheme is a simplified lateral view of the multilayer. Only one TbFeGa/TbFe interface is shown for simplicity. The size of the arrows represents the projection of the magnetic moments due to their rotation angle to form the DW. Black arrows are used for Fe magnetic moments, and red arrows for Tb.

Figure 3. Hysteresis loops at different temperatures for the nominal [TbFeGa(25 nm)/TbFe(50 nm)]$_2$ multilayer.

Figure 4. Hysteresis loops at 10 K for the nominal [TbFeGa(25 nm)/TbFe(50 nm)]$_2$ multilayer: (■) as-grown and (□) annealed.

Figure 1

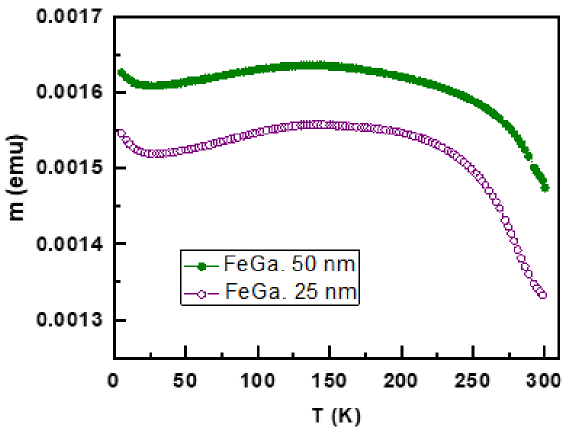
0.0017
0.0016
0.0015
0.0014
0.0013
m (emu)
0
50
100
150
200
250
300
T (K)
FeGa. 50 nm
FeGa. 25 nm

Figure 2

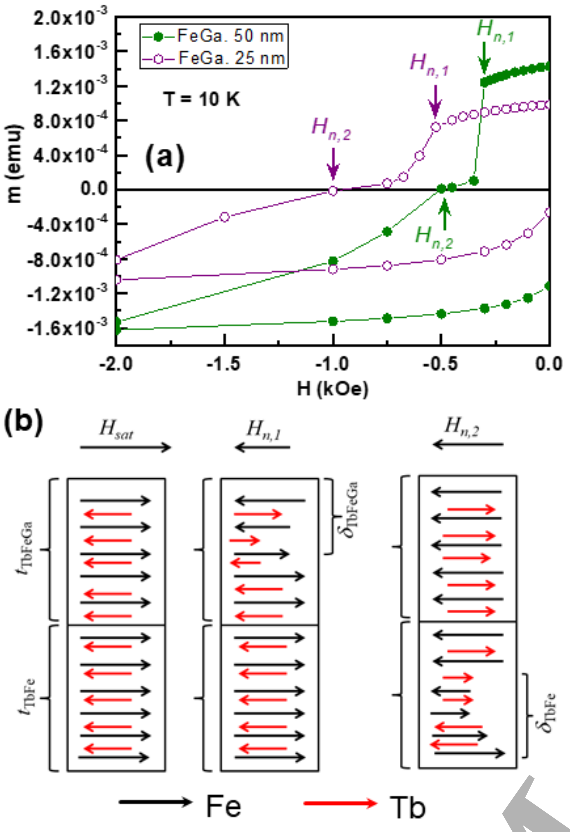
FeGa. 50 nm
FeGa. 25 nm
T = 10 K
(a)
m (emu)
H (kOe)
$H_{n,1}$
$H_{n,2}$
(b)
H_{sat}
$H_{n,1}$
$H_{n,2}$
t_{TbFeGa}
t_{TbFe}
δ_{TbFeGa}
δ_{TbFe}
Fe
Tb

Figure 3.

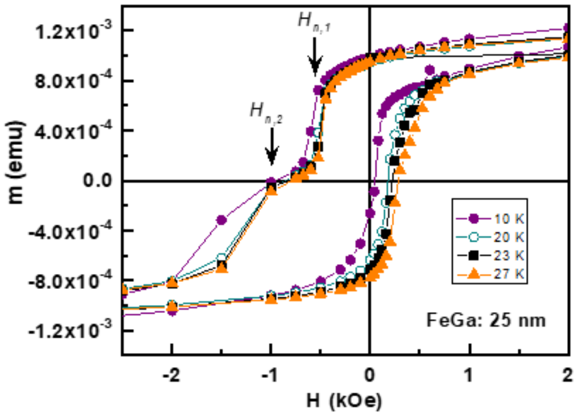
$H_{n,1}$
$H_{n,2}$
1.2x10^{-3}
8.0x10^{-4}
4.0x10^{-4}
0.0
-4.0x10^{-4}
-8.0x10^{-4}
-1.2x10^{-3}
m (emu)
10 K
20 K
23 K
27 K
FeGa: 25 nm
-2
-1
0
1
2
H (kOe)

Figure 4.

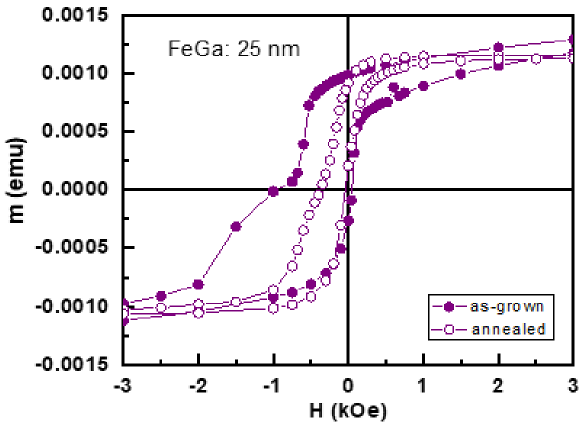
FeGa: 25 nm
m (emu)
H (kOe)
as-grown
annealed
0.0015
0.0010
0.0005
0.0000
-0.0005
-0.0010
-0.0015
-3
-2
-1
0
1
2
3